Available online at www.sciencedirect.com
ScienceDirect
Nuclear Instruments and Methods in Physics Research B 266 (2008) 4368–4372
NIM B
Beam Interactions with Materials & Atoms
www.elsevier.com/locate/nimb

Characterization of the LISOL laser ion source using spontaneous fission of ^{252}Cf

Yu. Kudryavtsev *, T.E. Cocolios, J. Gentens, O. Ivanov, M. Huyse, D. Pauwels, M. Sawicka, T. Sonoda, P. Van den Bergh, P. Van Duppen

Instituut voor Kern- en Stralingsfysica, Katholieke Universiteit Leuven, B-3001 Leuven, Belgium

Available online 5 June 2008

Abstract

A spontaneous fission Californium-252 source was placed inside a gas cell in order to characterize the LISOL laser ion source. The fission products from ^{252}Cf are thermalized and neutralized in the plasma created by energetic particles. Two-step selective laser ionization is applied to produce purified beams of radioactive isotopes. The survival of fission products in a single charge state has been studied in argon as a buffer gas for different elements.

PACS: 25.85.Ca; 32.80.Fb; 41.85.Ar

Keywords: Laser resonance ionization; Spontaneous fission; Californium-252; Ion catcher

1. Introduction

The LISOL laser ion source is used already for more than a decade for the on-line production of short-lived radioactive isotopes. The operational principle of the ion source is based on the element-selective multi-step laser resonance ionization of nuclear reaction products thermalized and neutralized in a high-pressure noble gas [1–4]. The laser ion source made it possible to perform β and γ decay studies of nuclei that are produced in proton-induced fission of ^{238}U [5] and in light/heavy ion-induced fusion evaporation reactions [6,7]. Resonant laser ionization was also used to characterize the laser ion source whereby a highly energetic (185 MeV) ^{58}Ni beam was stopped in the gas cell and converted into a low energy mass separated beam [8].

Recently, a ^{252}Cf fission source (0.78 mCi) was placed in a new gas cell in order to characterize the system and to study the survival of the fission products in atomic and ionic form in different experimental conditions. In this case, high energetic fission products are stopped in the argon buffer gas and are neutralized in the plasma created by ionizing particles. Purified beams of radioactive isotopes were produced using two-step laser resonant ionization via autoionizing states. The paper reports on the results obtained with this new set-up.

2. Experimental set-up

The spontaneous fission ^{252}Cf source allows to thermalize different fission products inside the gas cell. It has a half-life of 2.645 years and decays by alpha decay (96.9%) and spontaneous fission (3.1%). The source activity (on 21 April 2004) was 28.9 MBq. The yield of primary fission products is well determined [9]. Fig. 1 shows the independent yield of all fission isotopes in the mass range of 85–155. In the low mass region, the maximum yield corresponds to technetium isotopes, while in the high mass region to cesium and barium ones. The energy of the fission product lies around 105 MeV and 80 MeV for low- and high mass maximum, respectively.

The californium-252 source is located on a stainless steel substrate of 10 mm in diameter in the form of Cf–Pt alloy, Fig. 2. The active spot diameter is 4 mm. The source is

* Corresponding author. Tel.: +32 16 327271; fax: +32 16 327985.
E-mail address: yuri.kudryavtsev@fys.kuleuven.be (Yu. Kudryavtsev).

0168-583X/$ - see front matter © 2008 Elsevier B.V. All rights reserved.
doi:10.1016/j.nimb.2008.05.037

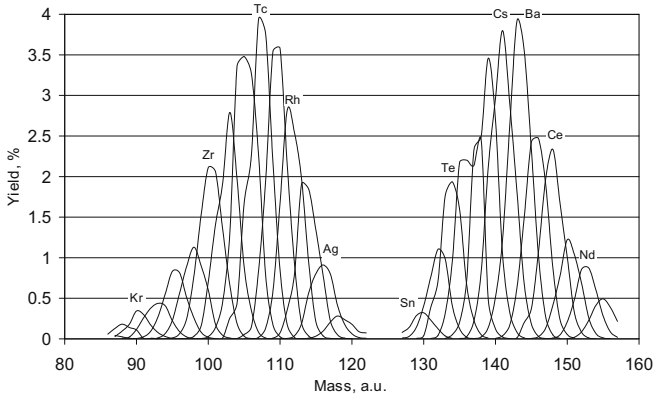

Fig. 1. The independent yield of fission isotopes in the spontaneous fission of ^{252}Cf [9].

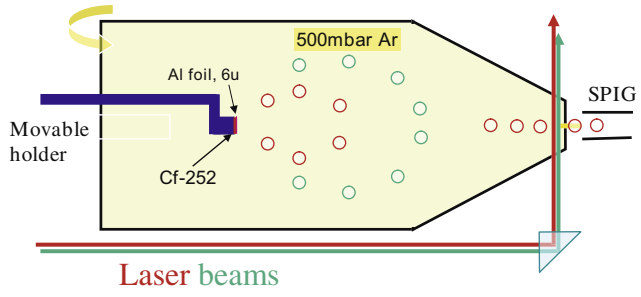

Fig. 2. Layout the gas cell with the spontaneous fission source ^{252}Cf.

placed on a moveable holder that allows changing the distance to the exit hole of the gas cell and its position relative to the cell axis. By measuring the energy of alpha particles emitted by ^{252}Cf it was concluded that the source is located at the distance of 0.1 μm from the surface and the emitted fission products are almost mono energetic. To reduce the energy of fission products, a 6 μm aluminum foil is placed above the source. Using the SRIM code [10], it was calculated that 34% of fission products are fed into the gas which corresponds to 5.3×10^5 atoms/s (November 2004).

The gas cell is made of aluminum and has an inner diameter of 7 cm and a length of 16 cm. It has a conical shape towards the exit hole, Fig. 2. The exit hole diameter is equal to 0.5 mm. The average evacuation time depends on the place where the fission products are stopped and equals to 2.7 s and 9.2 s at the distance of 52 mm and 100 mm to the exit hole, respectively. High purity argon gas, purified down the ppb level in a getter-based purifier, was fed into the gas cell from the back site.

All fission products can be stopped inside the gas cell at argon pressure of 500 mbar. Fig. 3(a) shows the calculated distribution of rhodium and cesium along the cell axis. Since cesium ions have a smaller initial energy and a bigger stopping power they have a shorter range in argon. All rhodium ions (6800 ions calculated) are stopped within a distance of 3.5 cm and cesium atoms within a distance of 2.7 cm. The rhodium ion distribution in a plane perpendicular to the cell axis is shown in Fig. 3(b). The radial distribution (4 cm) is less than the inner diameter of the cell. The stopping range of alpha particles emitted by ^{252}Cf is more than a factor of 2.5 larger and part of them is implanted in the cell wall. The plasma density created by the fission products and the alpha particles is estimated to be around 10^8 ion–electron pairs/cm^3. The recombination time in argon at this density equals to 0.1 s [8]. This is much shorter than the evacuation time of the thermalized fission products. The neutral atoms are transported by the gas flow towards the exit hole region where they can be ionized by laser beams, Fig. 2. A two-step scheme is used for the selective laser ionization of the neutralized fission products. The diameter of the laser beams inside the ion source is between 4 and 6 mm. The laser optical system consists of two dye lasers pumped by two time synchronized XeCl (308 nm) excimer lasers running with a maximum repetition rate of 200 Hz. The dye laser pulse length equals to

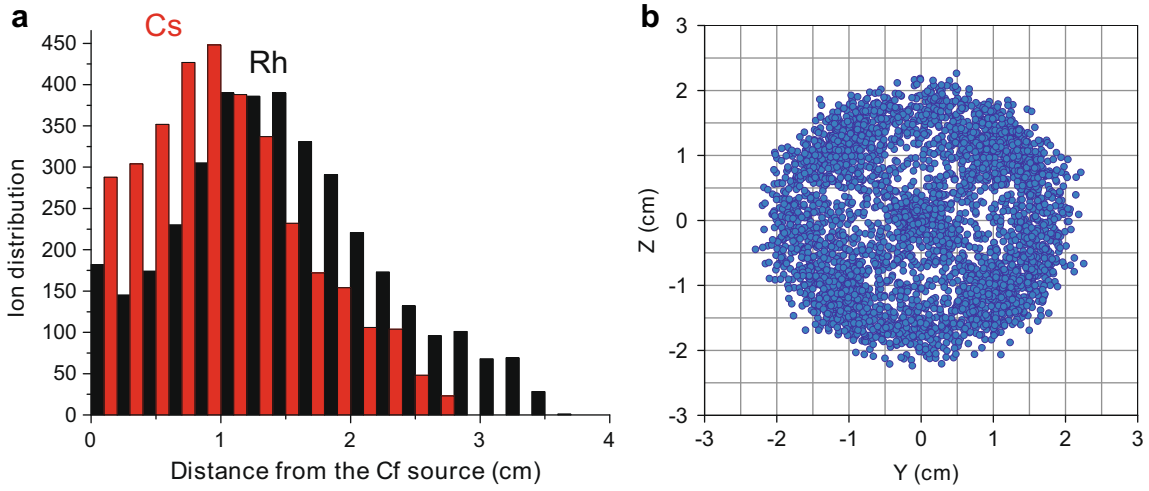

Fig. 3. (a) Distribution of cesium (gray) and rhodium (black) ions along the cell axis at 500 mbar argon. (b) Rhodium ion distribution in the plane perpendicular to the cell axis at 500 mbar Ar.

15 ns and the bandwidth equals to 0.15 cm^{-1}. To get UV light, the frequency of the first step laser radiation is doubled in the second harmonic generator. The dye laser beams are directed to the ion source located at a distance of 15 m where the two laser beams are overlapped at a small angle. Laser-produced ions are captured within the SextuPole Ion Guide (SPIG) [11] and are directed towards the mass separator. The mass separated beam is transported and deposited on a tape. The implantation point is surrounded by three plastic ΔE β detectors and two high purity Ge detectors for γ-detection.

3. Results and discussion

Different types of experiments can be performed using the ^{252}Cf source inside the laser ion source. First of all, the selective laser ionization provides yield enhancement of the desired isotopes. This gives the possibility to perform nuclear spectroscopy studies of exotic isotopes that are overwhelmed by more abundant isotopes. Also, the absolute laser ion source efficiency can be measured since the number of fission atoms fed into the gas is known. Without laser ionization, the survival of ions of different elements that have different chemical properties can be studied and by comparing the survival efficiency of ions with different half-life of the same element the evacuation properties of the gas cell can be evaluated.

3.1. Selective laser enhancement

Fig. 4 shows the yield of ^{112m}Rh isotopes (November 2004) after mass separation as a function of the distance between the ^{252}Cf and the exit hole when lasers are tuned on resonance with rhodium atoms and when lasers are off. To extract the production rates, the intensity of the 560 keV γ line, that is characteristic for the decay of the high-spin isomeric state of ^{112}Rh [12,13] was used. The points corresponding to the OFF case is a measure for the survival of rhodium ions in argon while the points corresponding to the ON case are dependent on the presence of neutral rhodium atoms, available for the laser ionization. For both cases the yield drops at small distance because part of the fission fragments are implanted in the wall. At a distance larger than 30 mm, the off-resonance production rate drops while the on-resonance production rate still increases even up to a distance of 50 mm. The former is mainly due to the recombination of the ions. At large distances the on-resonance production rate drops smoothly. This can be understood as due to the decay of ^{112m}Rh inside the gas cell ($T_{1/2} = 6.8$ s). The enhancement of the production rate due to resonant laser ionization at the distance of 52 mm equals to 160. The production rate of the ground state rhodium isotopes was measured using the 777 keV γ line. The total production of ^{112}Rh isotopes at a source to exit hole distance of 52 mm is 250 atoms/s, which corresponds to an overall efficiency of 3.75% defined as the number of ^{112}Rh atoms found after mass separation over the ones fed into a buffer gas. In the mass range 108–114, the mass separated ion current rate without lasers was less than 5 ions/s. This allowed us to measure the yield of the laser-ionized radioactive isotopes by direct counting the ions after mass separation. In this case, the ground and metastable states of ^{112}Rh cannot be distinguished. The yield of rhodium isotopes in this mass range measured by this counting technique was in agreement with the one deduced by the radioactive decay studies and the distribution in mass corresponded to the theoretical one [9].

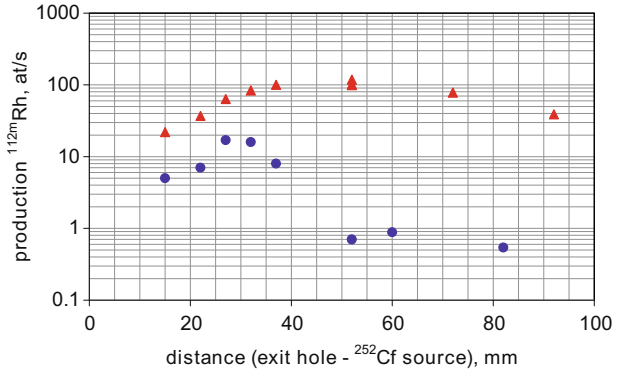

Fig. 4. Production of ^{112m}Rh isotopes as function of the distance between the ^{252}Cf source and the exit hole of the gas cell when lasers are tuned on resonance with rhodium atoms (triangles) and when lasers are off (circles).

3.2. Nuclear spectroscopy

If the isotope of interest is overwhelmed by more abundant isotopes, the laser enhancement can be very useful for its identification. As example, the β–γ spectroscopy of ^{116}Rh has been performed using the ^{252}Cf source. As can be seen from Fig. 5, the ^{116}Rh is produced in much smaller quantities than the Pd, Ag and Cd isobars. Fig. 6 shows a β-gated gamma spectrum obtained at mass 116. The line at 340 keV is present only when the lasers are on resonance

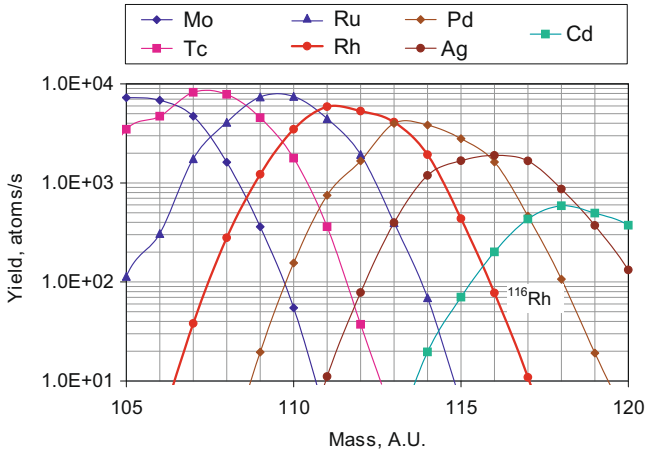

Fig. 5. Calculated yield of fission isotopes (September 2005) in the mass range 105–120 from ^{252}Cf [9].

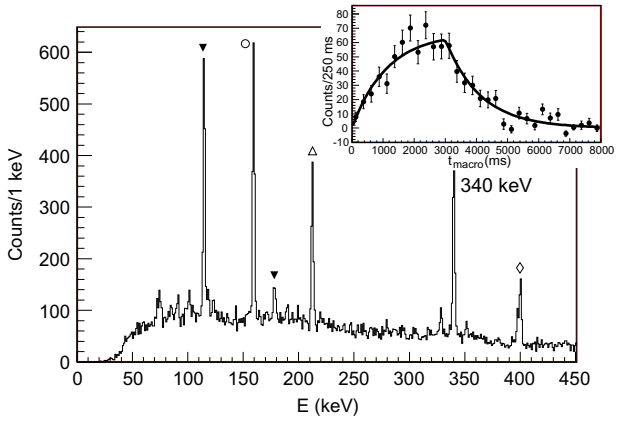

Fig. 6. β-gated γ spectra at mass 116 with lasers tuned on resonance with rhodium atoms (▼-^{116}Pd, ○-^{100}Nb, △-^{100}Y, ◇-^{100}Zr), the inset shows a growing-decay curve of 340 keV γ line.

with rhodium ($\lambda_1 = 232.258$ nm, $\lambda_2 = 572.55$ nm [1]). Since niobium, yttrium and zirconium ions form oxides very efficiently, gamma rays of ^{100}Nb, ^{100}Y and ^{100}Zr are present in the spectrum of mass 116. The intensity of the ^{116}Rh line is comparable with that of the oxides; however, it has to be stressed that the calculated yield of ^{100}Y, ^{100}Nb and ^{100}Zr are, respectively, 16 times, 19 times and 57 times larger than the yield of ^{116}Rh. To get information on the time behavior of the gamma rays, the implantation is performed in a cycle 3 s beam ON – 5 s beam OFF. The insert on Fig. 6 shows a growing-decay curve of 340 keV γ line intensity. Based on this behavior, a half-life $T_{1/2} = 787(38)$ ms was obtained [14]. This line is fed by the high-spin and the low-spin β decay of ^{116}Rh [15]. This value is larger compared to the previously reported half-lives for the high-spin isomer ($T_{1/2} = 0.57(5)$ s [15]) and low-spin isomer ($T_{1/2} = 0.68(6)$ s [16]). The available data do indicate a substantial feeding of the high-spin isomer in the present experiment but a precise ratio for the population of the high-spin versus low-spin isomer could not be determined.

3.3. Survival of ions in argon gas

Nowadays, gas cells are frequently used as gas catchers behind fragment separators [17–19]. Usually hePlium is used to stop recoils. Argon has a much higher stopping power and can be used instead of helium. However, ions form molecular adducts with argon much faster leading to losses in sidebands [4]. Ion recombination in argon is also much faster than in helium. The spontaneous fission ^{252}Cf source gives us an opportunity to study the ion behavior of different atomic ions in noble gases. For this, the ^{252}Cf source is placed in the standard LISOL laser ion source gas cell and the surviving ions extracted from the gas cell and mass separated are measured by means of their respective β decay. Comparing this production rate to the yields of the californium source gives the efficiency of survival of ions in this particular buffer gas cell filled with 500 mbar argon.

This gas cell is much faster than the one shown on Fig. 2. The average evacuation time of the stopped fission products is about 200 ms. The gas cell is made of a stainless steel and it is 5 cm in diameter. The ^{252}Cf source is placed on a mount attached to the side flange. Its position is chosen to be 32 mm, which corresponds to the maximum for the off-resonance production of rhodium, see Fig. 4. The argon gas is purified in a getter-based purifier to the sub-ppb level. The production of each isotope is determined from the intensity of γ emissions following its β decay and the mass separated beam was periodically switched on and off to obtain growing-decay information. A correction is applied to deconvolute the production into direct feeding and feeding through parent decay; isotopes for which in-cell decay from a parent nuclide would have been a major contribution, have been discarded from this study in order to limit our study to fission-produced isotopes. Fig. 7 shows the efficiency of different elements extracted as singly charged ions from the cell. The efficiency is calculated for each measured isotope. The final element efficiency is the weighted average of the efficiency of its isotopes. The measured efficiencies range from 74% for cesium down to 0.03% for krypton. The highest efficiency of cesium can be related to the ionization potential, which is the lowest of all considered elements. Fig. 8 shows the yield and the efficiency of mass separated cesium isotopes in the mass range 138–145. The ratio of ions found on the tape after mass separation to the number of ions fed into the gas from the fission source is the same (40%) in the measured mass range. If we take into account the SPIG – (60%) and the mass separator – (90%) transport efficiencies, we obtain an efficiency of 74% for cesium ions in a single charge state. Actually, most of the ions produced through fission of ^{252}Cf tend to recombine quickly with plasma electrons created by alphas and energetic fission products (note that there are no electrical fields in the gas cell, which could collect electrons). As a consequence it might be that what we observe as singly

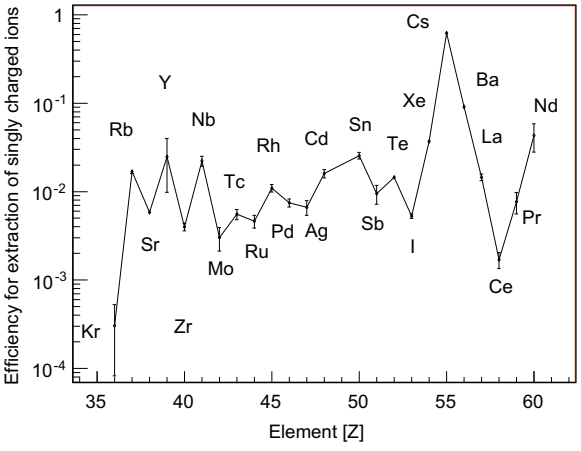

Fig. 7. Efficiency for extraction of fission fragments as singly charged ions from ^{252}Cf in 500 mbar Ar as a function of the element.

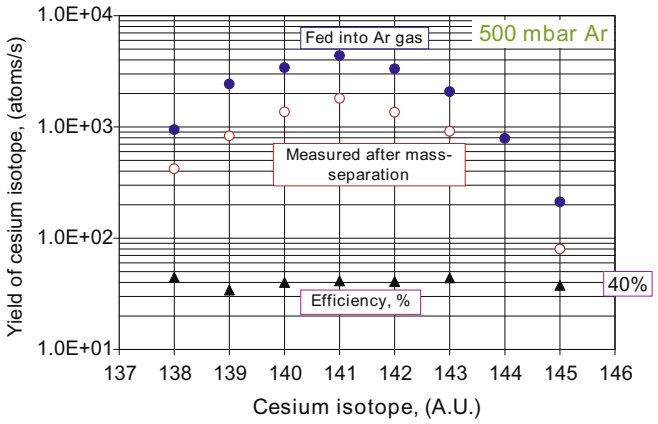

Fig. 8. Yield of Cs isotopes from ^{252}Cf in the mass range 138–145: open circles- measured after mass separation, filled circles- fed into argon gas (calculated [9]). The ratio gives the mass separated extraction efficiency of Cs isotopes.

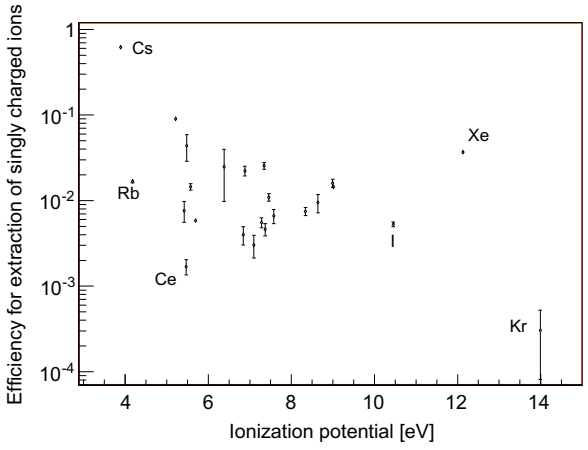

Fig. 9. Efficiency for extraction of fission fragments as singly charged ions from ^{252}Cf in 500 mbar Ar as function of the ionization potential.

charged ions is the result of survival of primary ions and re-ionization of the neutral atoms. It is difficult to explain the wide scattering of the efficiency values, but global as well as particular trends can be observed. Fig. 9 shows the efficiency of fission products extracted in a single charge state, as a function of the ionization potential. Apart from the results for Rb, Ce and Xe there is a general trend of smaller efficiencies for elements with a higher ionization potential, which might be explained if the re-ionization processes in the gas cell are important. However, other processes can also influence the efficiency. The high efficiency for xenon ions can be explained by Penning ionization; the ionization potential of xenon (12.13 eV) is close to the excitation energies of metastable argon atoms (11.55 eV and 11.75 eV). Also chemical reactions are not excluded.

4. Conclusions and outlook

A spontaneous fission ^{252}Cf source was used to characterize the gas cell for stopping of energetic fission products. The selective laser enhancement allows easy and reliable identification of isotopes that are overwhelmed by more abundant ones. The behavior of different ions and atoms in weekly-ionized argon plasma was investigated. As a following stage the influence of electrical field will also be studied.

Acknowledgement

This work was supported by the European Commission within the Sixth Framework Programme through I3-EURONS (contract no. RII3-CT-2004-506065), BriX-IUAP P6/23, FWO-Vlaanderen (Belgium) and GOA/2004/03.

References

[1] Yu. Kudryavtsev, J. Andrzejewski, N. Bijnens, S. Franchoo, J. Gentens, M. Huyse, A. Piechaczek, J. Szerypo, I. Reusen, P. Van Duppen, P. Van Den Bergh, L. Vermeeren, J. Wauters, A. Wöhr, Nucl. Instr. and Meth. B 114 (1996) 350.
[2] M. Huyse, M. Facina, Y. Kudryavtsev, P. Van Duppen, Nucl. Instr. and Meth. B 187 (2002) 535.
[3] Yu. Kudryavtsev, M. Facina, M. Huyse, J. Gentens, P. Van den Bergh, P. Van Duppen, Nucl. Instr. and Meth. B 204 (2003) 336.
[4] Yu. Kudryavtsev, B. Bruyneel, M. Huyse, J. Gentens, P. Van den Bergh, P. Van Duppen, L. Vermeeren, Nucl. Instr. and Meth. B 179 (2001) 412.
[5] S. Franchoo, M. Huyse, K. Kruglov, Yu. Kudryavtsev, W.F. Mueller, R. Raabe, I. Reusen, P. Van Duppen, J. Van Roosbroeck, L. Vermeeren, A. Wöhr, Phys. Rev. C 64 (2001) 054308.
[6] I. Reusen, A.N. Andreyev, J. Andrzejewski, N. Bijnens, S. Franchoo, M. Huyse, Yu. Kudryavtsev, K. Kruglov, W.F. Mueller, A. Piechaczek, R. Raabe, K. Rykaczewski, J. Szerypo, P. Van Duppen, L. Vermeeren, J. Wauters, A. Wöhr, Phys. Rev. C 59 (1999) 2416.
[7] S. Dean, M. Gorska, F. Aksouh, H. de Witte, M. Facina, M. Huyse, O. Ivanov, K. Krouglov, Yu. Kudryavtsev, I. Mukha, D. Smirnov, J.-C. Thomas, K. Van de Vel, J. Van de Walle, P. Van Duppen, J. Van Roosbroeck, Eur. Phys. J. A 21 (2004) 243.
[8] M. Facina, B. Bruyneel, S. Dean, J. Gentens, M. Huyse, Yu. Kudryavtsev, P. Van den Bergh, P. Van Duppen, Nucl. Instr. and Meth. B 226 (2004) 401.
[9] A.C. Wahl, At. Data Nucl. Data Tables 39 (1988) 138.
[10] J.F. Ziegler, J.P Biersack, <www.srim.org>.
[11] P. Van Den Bergh, S. Franchoo, J. Gentens, M. Huyse, Yu. Kudryavtsev, A. Piechaczek, R. Raabe, I. Reusen, P. Van Duppen, L. Vermeeren, A. Wöhr, Nucl. Instr. and Meth. B 126 (1997) 194.
[12] G. Lhersonneau, J.C. Wang, S. Hankonen, P. Dendooven, P. Jones, R. Julin, J. Äystö, Phys. Rev. C 60 (1999) 014315.
[13] L. Weissman, N.V.S.V. Prasad, B. Bruyneel, M. Huyse, K. Kruglov, Yu. Kudryavtsev, W.F. Mueller, P. Van Duppen, J. Van Roosbroeck, Nucl. Instr. and Meth. A (2002) 593.
[14] M. Sawicka et al., in press.
[15] Y. Wang et al., Phys. Rev. C 63 (2001) 024309.
[16] J. Äystö et al., Nucl. Phys. A 480 (1988) 104.
[17] M. Petrick et al., these proceedings.
[18] M. Facina et al., these proceedings.
[19] M. Wada et al., Nucl. Instr. and Meth. B 204 (2003) 570.